FAST ANALYSIS METHOD ASED ON POD-RBF SURROGATE MODEL

by

Yin WANG [a*], Meng-Huan WANG [b], Zhi-Qiang LIU [a], Na NI [c], and Bang-Yao ZHAO [a]

[a] Department of Engineering Mechanics, School of Civil Engineering and Architecture, Xi'an University of Technology, Xi'an, China
[b] Materials Genome Institute, Shanghai University, Shanghai, China
[c] Department of Engineering Mechanics, School of Science, Xi'an University of Architecture and Technology, Xi'an, China

Original scientific paper
https://doi.org/10.2298/TSCI2502361W

For the problems of large-scale non-linear finite element simulations, which often involve long computation times and difficulty in convergence, this paper presents an optimized method with good computational accuracy and applicability. First, a sufficient amount of data is obtained through finite element analysis or experiment, which is called a snapshot, and the principal components of the snapshot are extracted by using the proper orthogonal decomposition (POD) method. A low-order model of the physical problem is then established, and a low-order surrogate model of the complex problem is obtained by combining the radial basis function (RBF) method. This method can quickly predict the response with input data, which effectively shortens the computation time with good efficiency. The proposed method provides a new method in the computation of soft actuators.

Key words*: POD-RBF, surrogate model, soft actuators, non-linear*

Introduction

Soft robots are constructed from flexible or soft materials, enabling them to undergo continuous large deformations such as stretching, shrinking, bending, twisting, and folding. In comparison traditional robots, soft robots exhibit enhanced flexibility and safety [1]. They leverage the deformative characteristics of materials and structural designs to facilitate specific movements by altering the direction of material deformation. The designs are typically straightforward and easy to implement. Commonly employed in these designs are biomimetic structures inspired by artificial muscles [2], octopus tentacles [3], and deep-sea fish [4]. The driving mechanism primarily comprises fluid-driven pressure variation and deformation-based actuation utilizing smart materials.

To achieve precise control over soft robots for effective grasping and manipulation tasks, experimental design combined with finite element (FE) simulation has emerged as the principal approach for designing and optimizing soft actuators. Given the inherent characteristics of large deformation, non-linearity, and extreme redundancy in soft robots, it results in exponentially increasing simulation times during FE analysis. By implementing a surrogate

* Corresponding author, e-mail: wangyin@xaut.edu.cn

model instead of conducting numerous FE analyses, it is feasible to achieve response values with adequate precision and significantly reduced computation time.

Bhosekar *et al*. [5] discusses the advances in surrogate-based modelling, feasibility, analysis, and optimization. A surrogate model is essentially a mapping relationship between inputs and outputs. The applicable mapping relationships are as follows, polynomial interpolation, Kriging interpolation model, RBF, and ANN. This paper employs a combination of the POD technique and the RBF method to construct a surrogate model.

Fundamental principles of POD-RBF surrogate model

Proper orthogonal decomposition

The POD is a powerful method for facilitating the characterization of high dimensional physical processes through lower-dimensional representations. It is widely used in situations where model reduction is required. For large physical field data obtained through numerical simulations or experiments, which is called a snapshot matrix, POD will capture the dominant components of the snapshot matrix and reduce the amount of data storage required to describe the physical process.

Snapshot matrix represented by **U**, compute covariance matrix $\mathbf{D} = \mathbf{U}^\mathrm{T}\mathbf{U}$ or $\mathbf{C} = \mathbf{U}\mathbf{U}^\mathrm{T}$, then eigenvector, φ_j, and corresponding eigenvalue, λ_j, can be obtained by $\mathbf{C}\varphi_j = \lambda_j \varphi_j$.

The eigenvalues exhibit a rapid decay from the largest to the smallest, the cumulative contribution of the first K eigenvectors generally represents more than 95% of the total sum of all eigenvectors. Usually, the error of approximation is expressed using the ratio between kept eigenvalues and all of them, namely:

$$\frac{\sum_{i=1}^{K}\lambda_i}{\sum_{i=1}^{\text{all}}\lambda_i} \geq 95\% \tag{1}$$

The new basis is constructed of K eigenvectors that correspond to the first K largest eigenvalues of covariance matrix **C**. The $\bar{\mathbf{\Phi}}$ is the matrix that collects the first K eigenvectors, which correspond to the subspace of the reduce dimension and be written in the matrix form:

$$\bar{\mathbf{\Phi}} = [\varphi_j], \quad j=1, 2, \cdots, K \tag{2}$$

The function $U(x)$ can be written as a linear combination of a linear combination of K-basis functions $\varphi_i(x)$, namely:

$$U(x) \approx \sum_{i=1}^{K} a_i \varphi_i(x) \tag{3}$$

The coefficients a_i can be written in matrix form:

$$\bar{\mathbf{A}} = \bar{\mathbf{\Phi}}^\mathbf{T}\mathbf{U} \tag{4}$$

Radial basis functions

The RBF are frequently used when it is needed to construct an approximation of a certain multivariable function by interpolation between the existing data. The approach of RBF is different, and it seeks for one continuous function defined over the whole domain and that depends on the entire data set defined by the pairs of given, N, nodes and their values of the function. Therefore, the approximation of the function is written as a linear combination of some functions $g_i(x)$, that in general case can be non-linear functions:

$$f(x) \approx \sum_{i=1}^{N} \alpha_i g_i(x) \tag{5}$$

In this article, the linear splines RBF is chosen:

$$g_i(x) = \|x - x_i\| \tag{6}$$

The POD-RBF surrogate model

The approximation achieved in this way, is a discrete number of system responses, in this work, curvature U is already computed using the *full* model. From eq. (4), the coefficients matrix $\overline{\mathbf{A}}$ can be obtained. A further step to make a continuous approximation of the system over a certain parameter domain can be achieved if the POD is combined with the RBF interpolation. Choose the RBF interpolation $g_i(\mathbf{p}) = ||\mathbf{p} - \mathbf{p}_i||$, the matrix $\mathbf{G}$ and column vector $\mathbf{g}(\mathbf{p})$ can be calculated:

$$\mathbf{G} = \begin{bmatrix} g_1(\mathbf{p}_1) & g_1(\mathbf{p}_2) & \cdots & g_1(\mathbf{p}_M) \\ g_2(\mathbf{p}_1) & g_2(\mathbf{p}_2) & \cdots & \cdots \\ \cdots & \cdots & \cdots & \cdots \\ g_M(\mathbf{p}_1) & g_M(\mathbf{p}_1) & \cdots & g_M(\mathbf{p}_M) \end{bmatrix}, \quad \mathbf{g}(\mathbf{p}) = \begin{bmatrix} g_1(\mathbf{p}) \\ g_2(\mathbf{p}) \\ \cdots \\ g_M(\mathbf{p}) \end{bmatrix} \tag{7}$$

Solve $\overline{\mathbf{A}} = \mathbf{BG}$ to get coefficients of interpolation collected in matrix $\mathbf{B}$. The function $\mathbf{u}(\mathbf{p})$ of displacement depends on the shape parameter, K, taper angle, α, which is collected in vector, $\mathbf{p}$. For any vector of arbitrary parameters, $\mathbf{p}$, the approximation of response $\mathbf{u}(\mathbf{p})$ can be expressed:

$$\mathbf{u}(\mathbf{p}) \approx \overline{\mathbf{\Phi}}\mathbf{B}\mathbf{g}(\mathbf{p}) \tag{8}$$

Analysis of soft actuator with POD-RBF surrogate model

The finite element simulation of soft actuator

As shown in fig. 1(a), a single hollow internal chamber was placed along the length of the actuator at a fixed normalized distance from the outer radius of the actuator. The internal chamber was tapered in the same manner as that of the actuator. The cross-sectional shape of the chamber was annular with angle β = 120°, the outer radius of the annular is $R_i(z)$, and the inner radius is $R_m(z)$. The chamber was placed at a fixed normalized distance from the outer radius of the actuator, chamber placement, K, is defined [3]:

$$K = \frac{R_o(z)}{R_o(z) - R_i(z)} \tag{9}$$

where K is the constant that determines the relative position of the chamber cross-section with respect to the edge of the actuator's cross-section, as shown in fig. 1(a).

We identified the line running along the inner gripping side of the actuator, as the line – 1 shown in fig. 1(b). The red line is equally divided into 40 segments, each segment has its bent shape that determines the circle of radius, R_i, and the average curvature is calculated:

$$\kappa_i = \frac{1}{R_i} \; (i = 1, \cdots, 40) \tag{10}$$

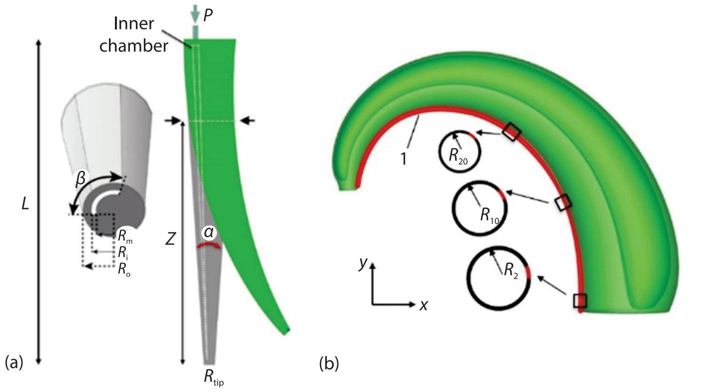

Figure 1. Geometry of the soft actuator; (a) cross-sectional view and side view and (b) schematic highlighting the procedure used to calculate the bending curvature along the length of the tapered actuator

When the pressure is applied to the inner surface of the cavity, the soft actuator bends towards the side opposite that of the cavity, as shown in fig. 2. In the FE simulation, 8-node linear brick elements (Abaqus C3D8H) are employed to construct the models. Gent hyperplastic material model is used by a user subroutine to calculate the response of the tapered soft actuators, with initial shear modulus $\mu = 195$ kPa and stiffening parameter $J_m = 12$. Each actuator was fixed at its base, the internal chamber was pressurized from $P = 0$ kPa to $P = 200$ kPa. During inflation, the deformed actuator at different pressures is shown in fig. 2. The shape parameter, K, taper angle, α, and fluid pressure, P, serve as direct factors influencing this bending curvature.

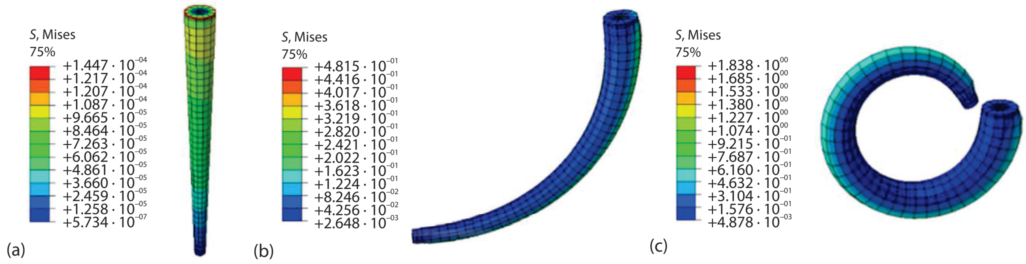

Figure 2. The FE simulation of the tapered actuator for $K = 2$ and $\alpha = 3°$; (a) P = 0 kPa, (b) P = 165 kPa, and (c) P = 200 kPa

Prediction of the average curvature with shape parameter

Parametric modelling with Python can obtain snapshot matrix. Using the POD-RBF method to predict the average curvature, they change with pressure of different shape parameters and taper angle independently.

Fixed taper angle precisely at $\alpha = 3°$, the external loop of the snapshot pertains to shape parameter K (from 2.0-3.3 with step 0.1), and the internal loop is for input pressure, P, (from 0-200 kPa with step 5 kPa), the numerical results of the average curvature as a function of shape parameter and input pressure, as shown in the heat map. Figure 3(a) shows the effect of K on the bending curvature by a fixed taper angle actuator, the results indicate that the bending curvature increases as the K increase.

Employ linear spline functions as RBF, the POD-RBF procedure is then employed to predict the average curvature changes with the pressure for $K = 2.7$, tab. 1. The FE result (solid line) was compared with those acquired by the POD-RBF method (dashed dot), as depicted in fig. 3(b), the POD-RBF result matches the numerical result well. The maximal relative error of the average curvature is only 0.81%.

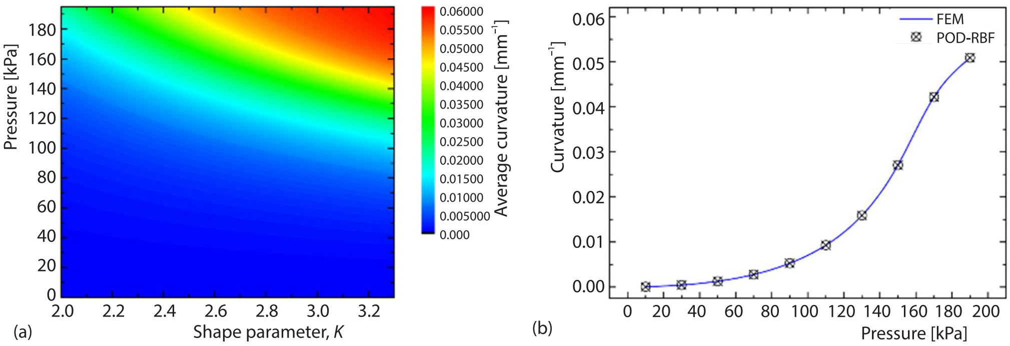

Figure 3. (a) Simulation results of the average bending curvature of the tapered soft actuators with taper angle α = 3° and (b) comparison of the average bending curvature between the numerical and POD-RBF of K = 2.7

Table 1. Simulation and POD-RBF results of bending curvature with shape parameter K = 2.7

Pressure [kPa]	FEM curvature [mm^{-1}]	POD-RBF curvature [mm^{-1}]	Relative error
10	$5.46 \cdot 10^{-5}$	$5.50 \cdot 10^{-5}$	0.81%
30	$4.66 \cdot 10^{-4}$	$4.67 \cdot 10^{-4}$	0.18%
50	0.0013	0.0013	0.00%
70	0.0028	0.0028	0.00%
90	0.0053	0.0053	0.00%
110	0.0093	0.0093	0.00%
130	0.0159	0.0159	0.00%
150	0.0271	0.0271	0.00%
170	0.0422	0.0422	0.00%
190	0.0509	0.0509	0.00%

Prediction of the average curvature with taper angle

We also investigated the effect of α on bending curvature by considering the actuator with K = 2. The external loop of the snapshot is by varying the taper angle, α, (from 3-9.5 with step 0.5), and the internal loop is for input pressure, P (from 0-200 kPa with step 5 kPa). The results in fig. 4(a) show the effect of, α, on the bending curvature by a fixed taper angle actuator, the results indicate that the bending curvature increases as the pressure increases, but decreases as the taper angle increases.

The POD-RBF procedure was employed to predict the average curvature changes with the pressure for α = 5.7°, which is beyond the sample points. Figure 4(b) shows the traditional FE result (solid line) matches the POD-RBF method (dashed dot) as well as the pressure increase. Table 2 provides the average curvature at various pressures with shape parameter K = 2 and taper angle α = 5.7°. The maximal relative error is only 1.64%. As the pressure rises, the relative error of both methods keeps decreasing constantly.

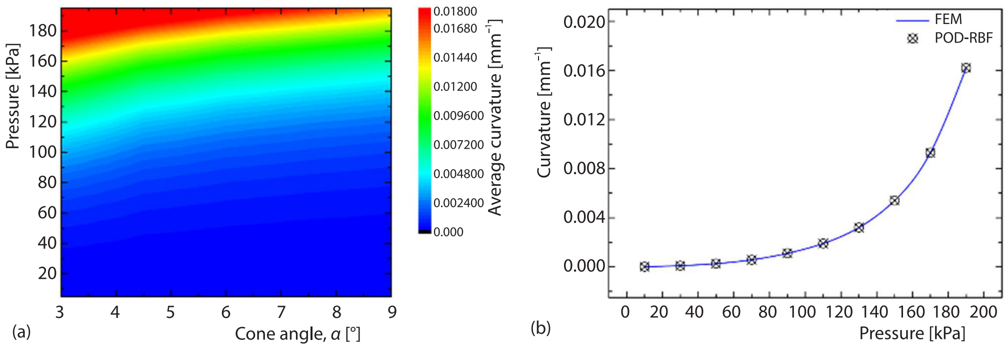

Figure 4. (a) Simulation results of average bending curvature of the tapered soft actuators with shape parameter *K* = 2 and (b) comparison between the numerical and POD-RBF of *α* = 5.7°

Table 2. Simulation and POD-RBF results of bending curvature with taper angle *α* = 5.7°

Pressure [kPa]	FEM curvature [mm^{-1}]	POD-RBF curvature [mm^{-1}]	Relative error
10	$1.12 \cdot 10^{-5}$	$1.14 \cdot 10^{-5}$	1.62%
30	$9.28 \cdot 10^{-5}$	$9.31 \cdot 10^{-5}$	0.27%
50	$2.62 \cdot 10^{-4}$	$2.67 \cdot 10^{-4}$	1.64%
70	$5.69 \cdot 10^{-4}$	$5.70 \cdot 10^{-4}$	0.09%
90	0.0011	0.0011	0.00%
110	0.0019	0.0019	0.00%
130	0.0032	0.0032	0.00%
150	0.0054	0.0054	0.00%
170	0.0093	0.0093	0.00%
190	0.0162	0.0162	0.00%

Conclusion

In the present report, we used a combination of POD and RBF methods to investigate the response of octopus-inspired soft actuators. Using the POD-RBF method to predict the average curvature, they change with pressure of different shape parameters and taper angle independently. By contrasting the computed results of bending curvature of octopus tentacles using POD-RBF and standard numerical simulation, the maximal relative error is only 1.64%, the method mentioned in this work can replace the traditional FE analysis of the soft actuators. While this study, only investigated the bending curvature, future work could also incorporate the stress and bending force. The method proposed in this paper could carried out completely and rapidly to explore the parameter design space, thus guide the design of soft robots.

Acknowledgment

This work was supported by the Natural Science Foundation of Shaanxi Educational Committee, China（2023-JC-YB-060）

Nomenclature

g – radial basis function, [–]
K – chamber placement, [–]

Greek symbols

α – taper angle, [°]
κ – bending curvature, [mm^{-1}]
λ – eigenvalue, [–]
$\bar{\mathbf{\Phi}}$ – subspace of the eigenvectors matrix, [–]

References

[1] Rus, D., *et al.*, Design, Fabrication and Control of Soft Robots, *Nature*, *521* (2015), 2, pp. 467-475
[2] Liu, Y., *et al*., A Light Soft Manipulator with Continuously Controllable Stiffness Actuated by a Thin McKibben Pneumatic Artificial Muscle, *IEEE/ASME Transactions on Mechatronics*, *25* (2020), 3, pp. 1944-1952
[3] Xie, Z., *et al*., Octopus Arm-Inspired Tapered Soft Actuators with Suckers for Improved Grasping, *Soft Robotics*, *7* (2020), 4, pp. 639-648
[4] Chen, X., *et al*., Self-Powered Soft Robot in the Mariana Trench, *Chinese Science Bulletin*, *67* (2022), 3, pp. 2697-2699
[5] Bhosekar, A., *et al*., Advances in Surrogate Based Modelling, Feasibility Analysis, and Optimization: A review, *Computers and Chemical Engineering*, *108* (2018), 1, pp. 250-267

Paper submitted: October 12, 2024
Paper revised: November 13, 2024
Paper accepted: November 23, 2024